CrossMark

ARTICLE

Low-temperature synthesis of high-purity boron carbide via an aromatic polymer precursor

Shujuan Wang, Yuefeng Li, and Xiaolong Xing
Department of Applied Chemistry, School of Science, Xi'an Jiaotong University, Xi'an, Shaanxi 710049, China
Xinli Jing[a)]
Department of Applied Chemistry, School of Science, Xi'an Jiaotong University, Xi'an, Shaanxi 710049, China; and Department of Applied Chemistry, MOE Key Laboratory for Nonequilibrium Synthesis and Modulation of Condensed Matter, Xi'an, Shaanxi 710049, China

(Received 22 February 2018; accepted 23 March 2018)

Boron carbide (B_4C) is an attractive material for numerous applications including vehicle armor, cutting tools, blasting nozzles, and abrasive powder, owing to its extreme hardness, high melting point, high Young's modulus, and excellent thermoelectric properties. However, the application of B_4C is limited by the high-temperature synthesis process. The present work aims to explore a low-temperature manufacturing process for synthesizing B_4C with a small amount of free carbon. Poly(resorcinol borate) with an aromatic structure and high char yield was chosen as the aromatic polymeric precursor. A combination of Fourier transform infrared spectroscopy, X-ray photoelectron spectroscopy, X-ray diffraction, scanning electron microscopy, transmission electron microscopy and Raman spectroscopy was performed to investigate the influences of the reaction temperature and holding time on the changes in the precursor microstructure. The results indicate that the rod-like structure of crystalline B_4C is successfully synthesized at 600 °C, and the free carbon can be reduced to about 0.8 wt% in the final product. This is because the pyrolysis temperature controlled the carbon content of the B_4C, which led to an enlarged contact domain between B_2O_3 and carbon, and a relatively low-temperature synthesis of B_4C.

I. INTRODUCTION

Boron carbide (B_4C) is a strong candidate for a variety of applications, including armor plating, blasting nozzles, abrasive wear-resistant materials, low-wear bearings, neutron moderators in nuclear reactors, and mechanical seal faces, as well as grinding and cutting tools,[1,2] due to its high melting point (2450 °C), high hardness (29.1 GPa), low density (2.52 g/cm^3), high elastic modulus (448 GPa), high-temperature stability, high neutron absorption cross-section (600 barns), and excellent high-temperature thermoelectric properties.[3,4] For these attributes, an extensive amount of research has been conducted over the past decade on producing B_4C powders. Methods of synthesizing B_4C can be classified as follows: (i) magnesiothermic reduction; (ii) carbothermic reduction; (iii) synthesis from elements; (iv) chemical vapor decomposition; and (v) synthesis from polymer precursors. However, commercial preparation of B_4C is still hampered by a lack of feasible production techniques suitable for industrial upscaling. Although fine B_4C powders can be obtained by the magnesiothermic reduction of B_2O_3 in the presence of carbon, this process is inadequate for the production of high-purity powders, as powders are easily contaminated by magnesium compounds.[5] The most commercially and industrially viable method for synthesizing B_4C is the carbothermic reduction of H_3BO_3 with carbon black at a temperature over 1750 °C in electric arc furnaces or graphite resistance furnaces.[6] However, the complete reaction of the carbon is very difficult due to the carbon monoxide produced as a by-product of the reaction. The carbon monoxide carries volatile boric species away from the reaction site, which breaks the stoichiometry, resulting in the final B_4C containing a considerable amount of free carbon residue. B_4C can also be synthesized from elemental boron and carbon directly, but the high cost of raw materials, high reaction temperature (>1500 °C), and long holding time have made this method economically unfavorable.[7] Chemical vapor deposition produces B_4C by reacting carbon or hydrocarbons using laser or plasma energy sources.[8] This results in the deposition of B_4C crystallites with high purity, high crystallinity degree, and excellent thermal stability. However, the high costs of the processing equipment and gaseous raw materials make this process unsuitable for the large-scale production of B_4C powder. Thus, while research on the preparation of B_4C has advanced tremendously over the last decade, it is still necessary to explore commercial preparation of B_4C with high purity and submicron size.

[a)]Address all correspondence to this author.
e-mail: xljing@mail.xjtu.edu.cn, rgfp-jing@mail.xjtu.edu.cn
DOI: 10.1557/jmr.2018.97

 © Materials Research Society 2018

https://doi.org/10.1557/jmr.2018.97 Published online by Cambridge University Press

As a result of these problems, several researchers have investigated alternative methods for producing B_4C. A promising alternative to high-temperature reaction techniques is the use of polymer precursors from inexpensive, nonhazardous, and readily available starting materials at lower temperatures.[9] First, the use of polymer precursors enables more homogeneous dispersion of the boron source (such as H_3BO_3, B_2O_3, or boron nitride[10]) and the carbon source at the molecular level, which aids in reducing synthesis temperature and carbon loss. Second, the use of polymer precursors allows for the precise control of the ceramic composition. Third, polymer precursors can undergo decomposition at lower temperatures, allowing for ceramic formation under milder conditions. All these factors contribute to a reduction in cost. In particular, borate esters of various polyols, e.g., poly(vinyl alcohol) (PVA), sugar,[11] mannitol,[12] glucose, citric acid, glycerol,[13] and sucrose,[14] have recently been studied as promising precursors for synthesizing B_4C. The formation of B–O–C bonds accelerates the dispersion of the boron source and the carbon source, leading to a reduction in synthesis temperature due to the enlarged surface-active area between B_2O_3 and carbon components with superior reactivity. Thus, this process can be carried out in the temperature range of 1000–1500 °C in a vacuum or inert atmosphere, which is lower than that of the general carbothermal reduction (2000 °C). For example, Wada et al.[15] reported the synthesis of B_4C from H_3BO_3 and glycerin precursor at 1300 °C for 4 h. However, the B_4C product contained a large amount of residual carbon. This is a common disadvantage of using organic precursors to synthesize B_4C. Sinha et al.[16] produced B_4C powder with a narrow size distribution and a median particle size of 2.25 μm by using citric acid and H_3BO_3 as raw materials. However, there was still 11.1 wt% free carbon left in the product. Yanase et al.[17] manufactured B_4C with less residual carbon using PVA and H_3BO_3. The precursor was first pyrolyzed in air at 600 °C for 2 h and then ground and heated at 1300 °C for 5 h under Ar flow. Kakiage et al.[18] synthesized crystalline B_4C without residual carbon by mixing equimolar amounts of H_3BO_3 and glycerine, then pyrolyzing at 1250 °C for 5 h in Ar flow. Nevertheless, as with other studies using polymeric precursors, a high pyrolysis temperature was needed. Mirabelli et al.[19] reported a production route of B_4C using poly(vinylpentaborane) as a precursor when heated at 1000 °C for 8 h in Ar flow. However, boranes are highly explosive, as well as expensive, making this process commercially unviable. Mondal et al.[20] proposed a low-temperature synthesis of B_4C powder from condensed BA–PVA product at a relatively low temperature of 800 °C for 2 h, but a large amount of unreacted boron oxide (B_2O_3) remained in the products.

Based on the above analyses, we conclude that the high synthesis temperature, the long reaction duration, and the large amount of residual carbon and B_2O_3 are the main deficiencies in synthesizing B_4C by using the polymeric precursor method. Moreover, it is difficult to grind the B_4C product into particle sizes fine enough for densification due to its extreme hardness. It is worth noting that aliphatic carbon resources are generally used when synthesizing B_4C using the polymeric precursor method. Although the reaction temperature between the aliphatic alcohol and H_3BO_3 is low, the carbonization of the resin backbone needs a high operating temperature and a long reaction time. This leads to an inevitable volatilization of B_2O_3 (melting point 450 °C) at high temperatures before the formation of B_4C,[21] thus leaving a high amount of residual carbon in the B_4C. Therefore, it is desirable to find a polymer precursor that can be charred at low temperature.

On this basis, the present paper proposes the synthesis of B_4C with a small amount of free carbon and B_2O_3 at a low temperature using an aromatic phenolic compound. Basically, resorcinol instead of aliphatic alcohol was adopted to react with H_3BO_3 synthesizing poly(resorcinol borate) (PRB) using the "three-stage stepwise temperature method". Our previous work[22] demonstrated that PRB consisted of aromatic, Ph–O–B, and B–O–B structures, as well as a small number of boron hydroxyl (B–OH) groups and phenolic hydroxyl (Ph–OH) groups. The unique structural characteristics of PRB showed great potential in synthesizing B_4C at a lower temperature. First, PRB exhibited excellent thermal resistance, and the char yield at 800 °C in a nitrogenous atmosphere reached as high as 69%. Second, the formation of B–O–C bonds by the dehydration reaction accelerated the dispersion of the boron source and the carbon source. Notably, B_2O_3 was formed during pyrolysis by the cleavage of borate O–C bonds,[23] which led to an enlarged contact domain between B_2O_3 and carbon, and was beneficial to the low-temperature synthesis of B_4C. Therefore, the objective of this work is to explore a simple and economical way to synthesize crystalline B_4C with little residual free carbon. First, thermogravimetric analysis (TGA) was performed to investigate the thermal degradation behavior of PRB to help determine the optimized pyrolysis temperature. To remove excess carbon components in the product, pyrolysis of PRB in air was performed before the carbothermal reduction of the condensed product. Then, Fourier transform infrared (FTIR) spectroscopy, X-ray diffraction (XRD), X-ray photoelectron spectroscopy (XPS), scanning electron microscopy (SEM), and transmission electron microscopy (TEM) were conducted to investigate the effect of the pyrolysis temperature and holding time on the structure evolution of the polymeric precursor, as well as on the synthesis behavior of B_4C.

https://doi.org/10.1557/jmr.2018.97 Published online by Cambridge University Press

II. EXPERIMENTAL

A. Materials

Resorcinol, H_3BO_3, *N*-methyl-2-pyrrolidone (NMP), anhydrous ferric trichloride, cyclohexane, xylene, acetone, and ether were supplied by the Tianjin Chemical Reagent Company (Tianjin, China). All the reagents used in these experiments were of analytical grade.

B. Preparation of PRB

PRB was synthesized from resorcinol and H_3BO_3 (molar ratio 1:1) according to the following procedures.[24] Under a nitrogen atmosphere, resorcinol (0.2 mol, 22.02 g), anhydrous ferric trichloride, cyclohexane, and NMP were added to a four-necked round-bottom flask equipped with a magnetic stirrer, a thermometer, a reflux condenser, and a Dean–Stark trap. The temperature was gradually increased to 95 °C, followed by the gradual addition of an NMP solution of H_3BO_3 (0.2 mol, 12.37 g). The mixture was maintained at this temperature for 8 h. Cyclohexane was then replaced by xylene, and the temperature slowly was increased to 165 °C. Next, the reaction was refluxed for 8 h. The system was then heated to 200 °C with the concurrent removal of xylene and was refluxed at this temperature until no water was observed in the Dean–Stark trap. The residual solvents were removed under reduced pressure, after which the collected brown liquid oil was kept molten at 220 °C for 3 h to further increase the molecular mass. The heating was then stopped, and the resulting product poured into a polytetrafluoroethylene beaker. The crude product was dissolved in acetone and precipitated three times. The precipitate was collected by filtration, and the filter cake was washed with ether several times until the filtrate was colorless. The obtained filter cake was extracted with ether using a Soxhlet extractor for 48 h to remove the NMP residue and unreacted reagents. Finally, the purified product was collected and dried at 200 °C in a vacuum drying oven for 10 h, and the powder sample of PRB with a red-brown color was obtained. The obtained PRB was further carbonized at different temperatures (450, 500, 550, 600, 650, or 700 °C) to investigate its thermal degradation behavior.

C. Synthesis of B_4C

The PRB sample, as described in Sec. II.B, was placed in a graphite crucible and heated from room temperature to the target temperature for 2 h using an electric muffle furnace at a heating rate of 5 °C/min. Then, the PRB was carbonized for 2 h at 450, 500, 550, 600, 650, and 700 °C using a temperature-programmed muffle furnace in air. The muffle furnace was cooled from the set temperature to room temperature at a rate of approximately 2 °C/min using the same gas flow rate that was used for heating. In addition, the PRB was carbonized at 600 °C for different holding times (such as 2, 4, 6, 8, or 10 h). The obtained black precursors were ground with an agate mortar and pestle into powder form. Then, the formed B_2O_3 component was removed from the precursor powder by washing with hot ionized water. The residue product was dried at 60 °C for 4 h in a vacuum drying oven until a constant weight was obtained.

D. Materials characterization

TGA diagrams were created using a NETZSCH TG 209C (Netzsch, Germany), and the samples were heated from room temperature to 800 °C at a heating rate of 10 °C/min under a nitrogen atmosphere. XPS measurements were obtained using a Perkin-Elmer PHI-5400 system (Mg K_α X-ray source, Perkin-Elmer Corp., Waltham, MA) attached to a data acquisition system. FTIR spectra were recorded between 400 and 4000 cm^{-1} from KBr pellets using a Bruker Tensor 27 spectrophotometer (Bruker, Karlsruhe, Germany) with a resolution of 1.0 cm^{-1}. The base vacuum of this system was 6.0×10^{-8} torr. The spectra were referenced against the C1*s* peak at 284.5 eV. XRD patterns were recorded using a Bruker D8 Advance (Bruker AXS, Karlsruhe, Germany) with Cu K_α radiation ($\lambda = 0.154$ nm, 40 kV and 40 mA). Data were collected between 10° and 70° with a scanning speed of 2°/min. The B_4C peak intensity ratio $I_{B_4C}/(I_{B_4C} + I_C)$ of the products was estimated from the main peak intensities of B_4C [I_{B_4C}; (021) reflection at $2\theta = 37.8°$] and the carbon component (I_C; amorphous carbon at $2\theta = 23–27°$) in the XRD pattern.[25] The Raman spectra were recorded from 600 to 2000 cm^{-1} on a confocal Raman microprobe (HORIBA Jobin Yvon, France) using the 534-nm excitation line of an argon-ion laser. The morphology was characterized using scanning electron microscope (JSM-6700F SEM, JEOL Co., Ltd., Tokyo, Japan). Particle size distribution was measured using a laser particle size analyzer (Malvern-ZEN 3690, Malvern Instruments Ltd., U.K.). The particle size of B_4C was studied with a JEOL JEM-2100 high-resolution transmission electron microscope (HRTEM, 200 kV, JEOL Co., Ltd., Tokyo, Japan). The morphology was also determined on a JEM-3010 TEM, JEOL Co., Ltd., Tokyo, Japan. For TEM examination, the dried samples were ultrasonically dispersed in water and cast onto TEM grids.

III. RESULTS AND DISCUSSION

A. Thermal properties of PRB

The thermal decomposition processes of PRB were analyzed by TGA to deduce the optimum temperature range for the preparation of B_4C (Fig. 1). The results indicated that PRB exhibited excellent thermal performance, specifically with a high thermal decomposition temperature and a high char yield. As shown in Scheme

https://doi.org/10.1557/jmr.2018.97 Published online by Cambridge University Press

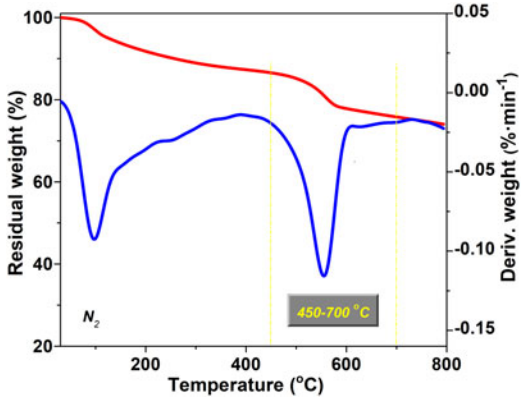


FIG. 1. TGA and DTG curves of PRB under a nitrogen atmosphere from room temperature to 800 °C at a heating rate of 10 °C/min.

S1, the molecular skeleton of PRB mainly consisted of aromatic structures, borates, B–O–B structures, and a small number of B–OH and Ph–OH groups (Table SI). The 5% and maximum weight loss temperatures ($T_{5\%}$ and T_{max}) of PRB were 226 °C and 440 °C (Table SII), respectively. The char yield of PRB (800 °C, N_2 atmosphere) reached 69.0%. According to the DTG curves, the degradation process of the PRB is predominantly divided into three stages. The first stage of thermal degradation, occurring from 200 to 450 °C, is mainly attributed to the release of adsorbed water and the dehydration reactions caused by the unreacted B–OH and Ph–OH groups in PRB. During the second stage of thermal degradation (450–700 °C), the destruction of the resin skeleton occurs. A significant mass loss (10.75 wt%) for PRB is observed at this stage. In this stage, the macromolecular chain breaks into smaller fragments, accompanied by the formation of B_2O_3, the release of water, CO_2, phenol, and methyl derivatives.[23] The third stage in the temperature range from 700 °C to the end of this experiment (800 °C) is a further cracking process of the resin residues, only 1.77 wt% of the total mass loss takes place at a lower rate in this stage. Therefore, we selected 450–700 °C as the optimum temperature range for the preparation of B_4C and studied the thermal cracking process occurring in this stage in detail.

B. Effect of pyrolysis temperature on the synthesis of B_4C

The structural evolution of PRB with increasing heat treatment temperatures was investigated by FTIR and XRD. FTIR measurements [Fig. 2(a)] were performed to evaluate the structural evolution of the main functional groups of PRB after treatment at different temperatures (450, 500, 550, 600, 650, or 700 °C). For PRB, the peaks at 3221 and 1600 cm^{-1} corresponded to the stretch vibrations of the boron hydroxyl O–H and aromatic ring, respectively. The characteristic bands at 706 and 798 cm^{-1} were assigned to the B–O stretching in B–O (B) and boroxine, respectively, generated by the dehydration of B–OH groups. The characteristic absorption band at 1315 cm^{-1} was assigned to the borate's B–O stretch vibration, and the appearance of the peak at 1444 cm^{-1} was due to the B–O stretching vibration. After heating at 450 °C for 2 h, the intensities of the B–O–C (1302 cm^{-1}) and aromatic ring stretching vibrations decreased, whereas the intensity of the absorption peak for boroxine at 798 cm^{-1} became stronger. Hence, we conclude that the O–C bond of the borate has been destroyed at an early stage of PRB pyrolysis (450 °C), with the accompanying formation of B_2O_3. After heat treatment at 550 °C for 2 h, the absorption bonds of the aromatic ring and borate's B–O stretch vibrations almost disappeared, and the intensities of the absorption peaks for B–O–B (706 cm^{-1}) and B–O (884 and 1444 cm^{-1}) decreased. [Fig. 2(b)] showed the XRD patterns of the products obtained via pyrolysis at different heat treatment temperatures of 450–700 °C for 2 h in air flow. XRD results showed that the crystalline diffraction peak of B_2O_3 (2θ = 14.1°, 28.2°) appeared in the pyrolysis products of PRB when the pyrolysis temperature was lower than 550 °C.[26] Therefore, as the heat treatment temperatures increase, the aromatic structures are converted to amorphous carbon, while the borate structures are gradually converted to B_2O_3,[27] both of which are the elements required for the synthesis of B_4C. As the temperature increased to 600 °C, a significant drop in the intensity of the diffraction peak of B_2O_3 was observed. In addition, the obvious diffraction pattern peaks at 33.3°, 35.5°, 38.9°, 52°, and 54.9°, attributed to B_4C,[28] appeared at 600 °C. FTIR analyses also revealed that the stretching vibration of the B–C bond was observed at 645 cm^{-1}[29] However, the diffraction pattern peak of B_2O_3 was not yet detected at this temperature. This further confirms the feasibility of synthesizing B_4C from the reaction of B_2O_3 with amorphous carbon at 600 °C, which is a significantly lower temperature than that reported for B_4C synthesis using a condensed product.[13]

It is known that the synthesis of B_4C powder is greatly affected by the differences in the dispersibility and homogeneity of the B_2O_3 and carbon components. Compared to the aliphatic precursor, the aromatic rings and borate structures of the PRB were gradually converted to amorphous carbon and B_2O_3,[30] respectively, during pyrolysis. Notably, PRB itself had some B–O–B structures. The pyrolysis of PRB enabled the formation of more B–O–B structures with high dispersibility at high temperatures. Such a condensed product yielded a precursor with a fine, homogeneous dispersion of B_2O_3/C. A finely dispersed structure increased the number of nucleation sites on B_4C, which was beneficial to the low-

https://doi.org/10.1557/jmr.2018.97 Published online by Cambridge University Press

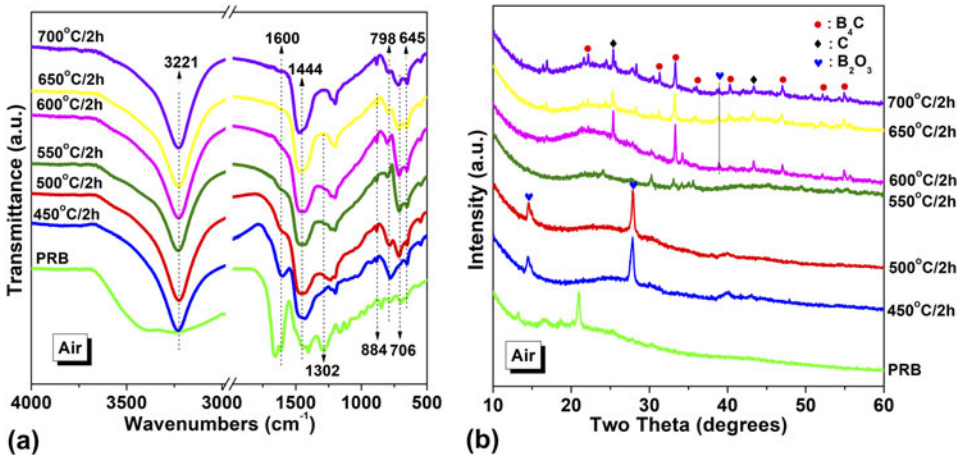


FIG. 2. FTIR spectra (a) and XRD spectra (b) of PRB and its pyrolysis products after heat treatment at different temperatures of 450–700 °C for 2 h in a muffle furnace under air atmosphere.

temperature synthesis of B_4C. When the pyrolysis temperature was higher than 600 °C, the pyrolysis products consisted entirely of B_4C and amorphous carbon (2θ = 25.3° and 43.4°). The peak at 2θ = 40.3°, attributed to B_2O_3, was also observed above 600 °C owing to the oxidation of partial B_4C. As reported by Kılıçarslan et al.[31] and Li et al.,[32] a B_2O_3 glass film was formed on the surface of the carbonization product of B_4C after pyrolyzed at 650 °C under an air atmosphere. As a result, the combined effect of the formation and oxidation of B_4C led to the small change in the intensity ratio of $I_{B_4C}/(I_{B_4C} + I_C)$. FTIR results indicated that the positions and intensities of the absorption peaks for the boron-containing functional groups remained unchanged. This may result from the synergistic effect of B–O–C bonds breaking and forming B_2O_3, and the formation of B_4C from B_2O_3 and amorphous carbon.

According to the carbothermal reduction reaction, the stoichiometric C/B_2O_3 ratio should be controlled at 3.5 to produce the highest amount of B_4C with less free carbon. The C/B_2O_3 ratio is calculated as follows. First, the sample is weighed, followed by the removal of B_2O_3. It is known that B_2O_3 is soluble in hot water and is therefore removed by submerging the pyrolyzed sample in 80 °C distilled water. After continuously stirring for 30 min, a solution containing carbon and dissolved B_2O_3 is obtained. The solid carbon is separated from the dissolved B_2O_3 solution to calculate the carbon content produced after pyrolysis. This is then subtracted from the original weight of the sample to give the amount of B_2O_3. SEM was used to investigate the state of the B_2O_3 and carbon components in the precursors. Moreover, the morphologies of the corresponding carbon structures, whose B_2O_3 component was removed by washing with hot water, are also shown in Fig. 3. It can be seen that B_2O_3 dispersed uniformly in the carbon matrix of the pyrolysis products [Figs. 3(a)–3(c)]. The result was in accordance with our previous results that the borate O–C bonds broke accompanying the formation of B–O–B structures. The width of B_2O_3 was approximately 100–200 nm according to the scale in the image. Besides, some voids were also observed on the surface of the pyrolysis products due to the volatilization of carbon dioxide, carbon monoxide, or other volatile compounds. As expected, B_2O_3 could not be detected after washing [Figs. 3(d)–3(f)], and correspondingly, the number of voids increased significantly, indicating that B_2O_3 was removed. When the pyrolysis temperatures increased, the number of pores on the surface of the carbonized product increased significantly.

The C/B_2O_3 molar ratios of the PRB after pyrolysis at different temperatures in air were calculated as shown in Fig. S1. The C/B_2O_3 ratios decreased with increasing heat treatment temperatures, and this phenomenon was attributed to the slight volatilization loss of B_2O_3 occurring during the heat treatment. It is evident that the C/B_2O_3 ratio (3.42) of the pyrolysis products at 600 °C is close to 3.5. Therefore, the thermal decomposition temperature was fixed at 600 °C, which was considered the most suitable temperature for the pyrolysis process, and the holding time was changed. This also suggested that strict compositional control of the precursor solely by controlling the thermal decomposition temperature was difficult, as increasing the pyrolysis temperature promoted the breakdown of the polymer chain.[33]

C. Effect of pyrolysis time on the synthesis of B_4C

Thermal decomposition of PRB at 600 °C for 4, 6, 8, and 10 h in air atmosphere was performed to determine the appropriate pyrolysis time for the formation of B_4C. Fig. 4(a) shows the change in the XRD patterns of the products obtained via heat treatment of the thermally decomposed products at 600 °C with holding time in air.

https://doi.org/10.1557/jmr.2018.97 Published online by Cambridge University Press

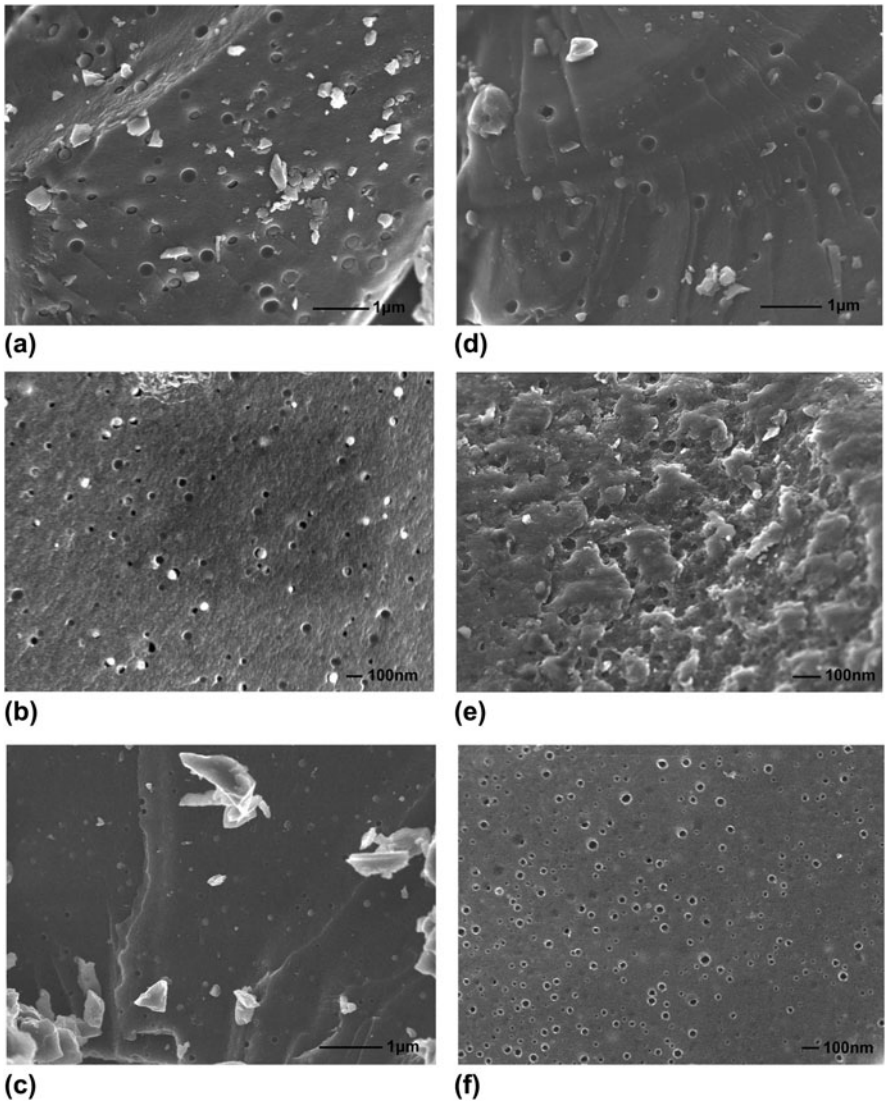


FIG. 3. SEM images of the surface morphology of the pyrolyzed products for PRB after heat treatment at 600 °C for 4, 6, and 8 h in air before (a–c) and after (d–f) the removal of B_2O_3.

The results indicated that the pyrolysis products of PRB mainly consisted of amorphous carbon (2θ = 24.5°, 25.4°, 43.4°), B_2O_3 (2θ = 14.5°, 28.2°, 40.3°), and B_4C (2θ = 31.3°, 33.3°, 38.9°, 52°, 54.9°). When the holding time was increased from 2 to 8 h, the intensity of the B_4C peak increased significantly, indicating the increase in the crystallinity degree of B_4C. The intensity ratio of $I_{B_4C}/(I_{B_4C} + I_C)$ showed little difference when increasing the pyrolysis time. We attributed this to the volatilization of B_2O_3 as well as to the oxidation of B_4C. FTIR measurements were conducted to evaluate the bonding state of the pyrolysis products of PRB [Fig. 4(b)]. When the holding time was lower than 8 h, the intensity of the absorption peak at 646 cm^{-1}, assigned to the B–C stretch vibration, gradually increased with increasing time, whereas the peaks at 881, 803, and 707 cm^{-1} corresponding to the B–O, boroxine, and B–O–B structures, respectively, became weaker. When the holding time further increased (above 8 h), no obvious changes in the intensity of the absorption peaks for B–C, B–O, boroxine, and B–O–B were observed. This phenomenon was in good agreement with the XRD results. Therefore, on the basis of shortening the pyrolysis time for the sufficient synthesis of B_4C, the optimum temperature is 600 °C and the optimum holding time is 8 h.

To obtain B_4C with high purity, the unreacted B_2O_3 was removed in hot water. Then, the structure and morphology of the pyrolysis products after removing B_2O_3 were investigated by XPS, FTIR, SEM, XRD, and TEM. XPS was used to examine the chemical surface compositions of the pyrolysis products of PRB after washing, and the assignments of XPS spectra based on

https://doi.org/10.1557/jmr.2018.97 Published online by Cambridge University Press

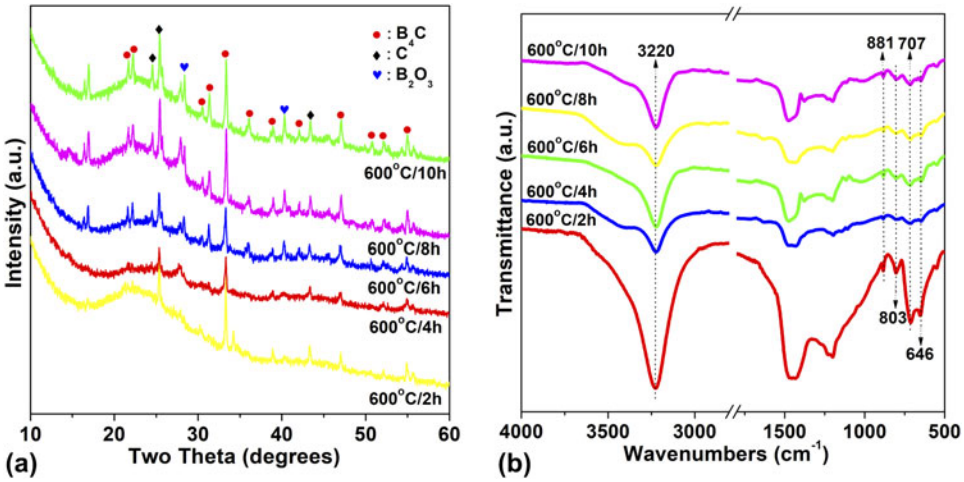


FIG. 4. The XRD spectra (a) and FTIR spectra (b) of the pyrolysis products of PRB obtained by heat treatment at 600 °C for different durations in a muffle furnace under air atmosphere.

the Lorentzian fitting are listed in Table SIII. The carbon, oxygen, and boron elements were detected from the full-scan XPS spectra (Fig. S2). Theoretically, if the carbon and produced B_2O_3 fully reacted, the B/C atomic ratio of B_4C should be equal to 4. In fact, the qualification of the peak intensity reveals that the atomic ratio of B to C for the pyrolysis products of PRB after washing is lower than 4, indicating a lower amount of boron content. This result suggests that the volatilization of B_2O_3 and its participation in the formation of B_4C occur simultaneously, prolonging the pyrolysis time at 600 °C. As a result, no obvious regular changes in the relative content of the B, O, and C elements are observed (Table I). The C1*s* XPS results suggested that the carbon atoms existed in four chemical states in the pyrolysis products of PRB. The peak at 283.4 eV was usually ascribed to the C–B bond in B_4C [Fig. 5(a)].[34] It is clear that the percentage areas of the C–B binding reached its maximum value after heating at 600 °C for 8 h [Fig. 5(b)]. The strong C–C bonding that originated from the sp^2 graphite structure appeared at 284.65 eV.[35] The observed signal from C–H bonding was observed at 285.5 eV compared with the pure carbon. The peak at 288.33 eV corresponded to the C=O bond, indicating the partial oxidation of the amorphous carbon. The high-resolution B1*s* XPS spectra indicated that the B atom existed in three different chemical environments. The low energy component at 189.51 eV was assigned to the nonstoichiometric B_4C [Fig. 5(c)],[34] which provided evidence for the synthesis of B_4C at the low temperatures. The observed signal at 192.18 and 190.18 eV were related to the B–O–B, and B–O bondings,[36] respectively. The percentage areas of the B–C binding clearly increased with increasing the pyrolysis time and reached the highest level at 8 h [Fig. 5(d)]. FTIR analyses showed that the characteristic absorption band at 803 cm^{-1} assigned to the B–O–B stretching vibration

TABLE I. Compositions of the pyrolysis products of PRB obtained from the XPS analyses after heat treatment at 600 °C for different durations in air after washing.

	Atomic ratio (wt%)		
Polymer	C	B	O
600 °C/2 h	74.92	3.72	21.36
600 °C/4 h	68.72	7.16	24.12
600 °C/6 h	67.61	8.73	23.66
600 °C/8 h	66.23	5.95	27.82
600 °C/10 h	68.42	2.37	29.21

almost disappeared after washing, leaving only the B–C stretching vibration at 646 cm^{-1} [Fig. 5(e)]. A closer examination revealed that the strength of the B–C stretching vibration reached its highest level after pyrolysis at 600 °C for 8 h, which provided a valuable basis for determining the pyrolysis conditions. It is important to note the appearance of the absorption peak at 3428 cm^{-1}, ascribed to the O–H stretching vibrations of water, which may be attributed to the existence of pore structures produced during pyrolysis that can hide the water molecules. Figure 5(f) shows the XRD patterns of products obtained by pyrolysis at 600 °C for different durations in air after washing. XRD results revealed that the peaks appearing at $2\theta = 33.4°$, 38.9°, 43.4°, 47.2°, and 55.1° corresponded to the crystalline diffraction peak of B_4C. The peak at $2\theta = 25.5°$ was ascribed to the crystal diffraction peak of graphite, and the intensity became weaker with increasing pyrolysis time. This is in accordance with the XPS and FTIR results that the pyrolysis products after washing mainly consist of B_4C. Consequently, it can be concluded that the breaking of B–O–C bonds during pyrolysis is important for achieving the low-temperature synthesis of B_4C, as the highly dispersed structure provides a larger surface-active area

https://doi.org/10.1557/jmr.2018.97 Published online by Cambridge University Press

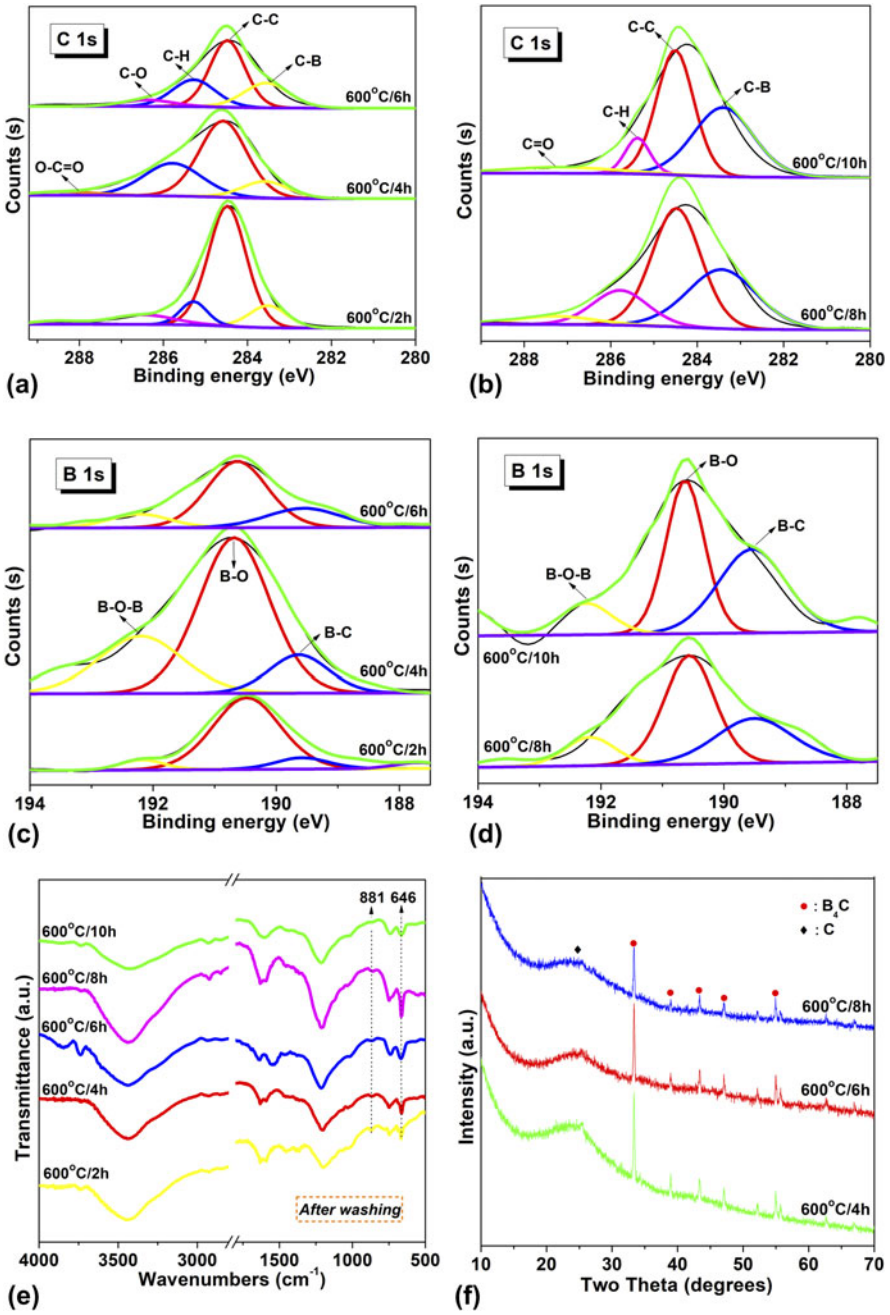


FIG. 5. The structure of the pyrolysis products of PRB obtained by heat treatment at 600 °C for different durations in air after washing: (a and b) C1 XPS spectra, (c and d) B1 XPS spectra, (e) FTIR spectra, and (f) XRD spectra.

between the B_2O_3 and carbon components with superior reactivity to obtain B_4C with less free carbon.

The residual free carbon in the formed B_4C was determined by the following methods.[25] An amount of B_4C powder containing some free carbon was weighed and taken as W_1. It was then heated to 700 °C for 30 min in air. It was assumed that all free carbon and part of the B_4C powder were oxidized during the heat treatment. Thus, the remaining powder, W_2, was washed with hot water to remove the oxidized part of the B_4C, namely, B_2O_3. The resulting powder was then dried and weighed as W_3. The different $W_2 - W_3 = W_4$ yielded the amount of B_2O_3, and therefore also yielded the oxidized B_4C (W_5). The sum of $W_3 + W_5 = W_6$ gave the total B_4C, and therefore the different $W_1 - W_6 = W_7$ yielded the amount of residual free carbon. The calculation results indicated that increasing the holding time led to a decrease in free carbon, and the B_4C powder contained only 0.82 wt% of free carbon after pyrolysis at 600 °C for 8 h. All these results confirm the rationality of determining the pyrolysis time as 8 h. As reported by Kakiage et al.,[12] thermal decomposition of a condensed product in air before

https://doi.org/10.1557/jmr.2018.97 Published online by Cambridge University Press

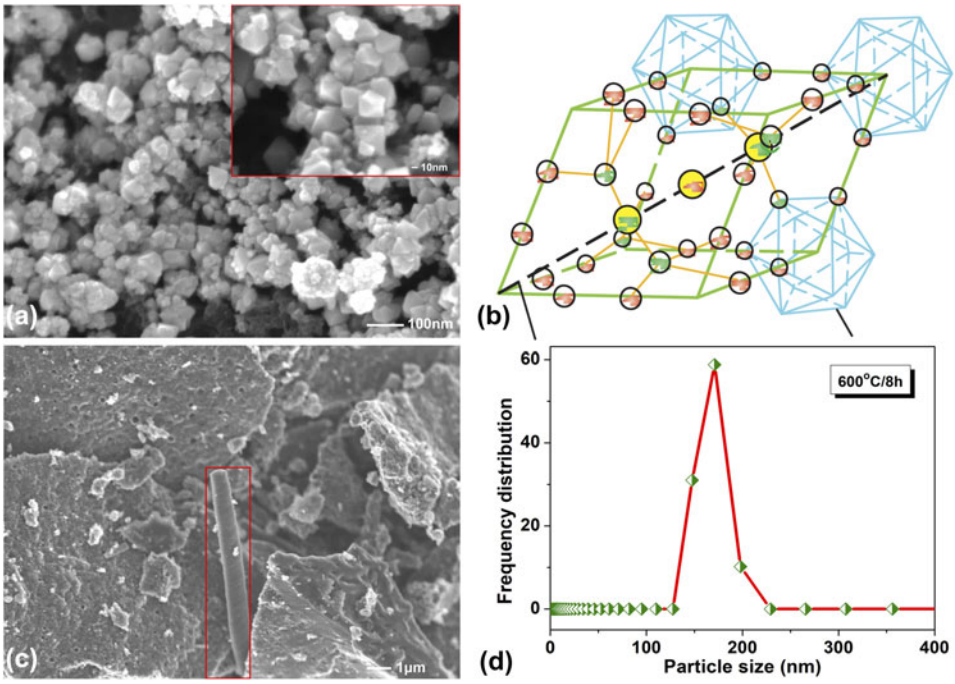


FIG. 6. (a and c) SEM spectra of the prepared B_4C, (b) unique atomic structure of B_4C, and (d) particle size distribution of the pyrolysis products of PRB after being treated at 600 °C for 8 h in an air flow after washing.

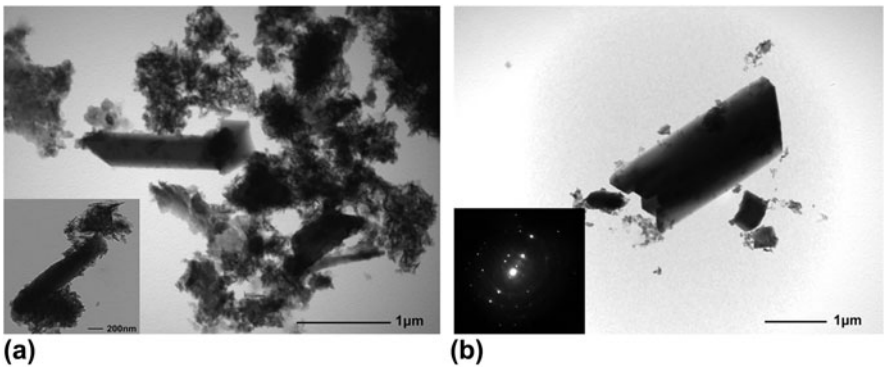


FIG. 7. TEM image (a) of the single B_4C rod-like particle and its ED pattern (b).

carbothermal reduction resulted in the removal of residual free carbon, and B_4C powder with less free carbon was obtained at a lower temperature. Based on the above analyses, we conclude that heating temperature and holding time are observed to have profound influence on the B_4C formation. This result is also reported by Weimer et al. Finally, it is clarified that the PRB is a promising precursor for the preparation of B_4C with little free carbon at a low temperature.

The morphology of the B_4C powder produced using the optimum process conditions (600 °C/8 h) was analyzed by SEM and TEM. The SEM images [Figs. 6(a) and 6(c)] showed that the prepared B_4C was icosahedral particles or rod-like shape, which provided the evidence that B_4C was successfully synthesized. Generally, the unique atomic structure of B_4C consists of distorted $B_{11}C$ icosahedra,[37] located at the corners of a unit cell of a rhombohedral lattice [Fig. 6(b)], connected along the (111) axis by atomic linear C–B–C chains.[3] TEM images of the sample revealed that the B_4C crystallite was composed of rod-like particles, which was commonly produced during carbothermic reduction of B_2O_3. The B_4C rod-like particles had diameters of approximately 200 nm [Fig. 7(a)] and lengths of approximately 1 μm [Fig. 7(b)]. The inserted ED pattern was consistent with high crystallinity. The particle size distribution of the B_4C powder was determined by using a particle size analyser. For the general carbothermal reduction reaction, the synthetic materials of carbon powder and B_2O_3 possess high crystallinity. The formation of B_4C is equivalent to the process of replacing O atoms in B_2O_3 by C atoms, and finally the B_4C with larger particle size is formed. Herein, the formed B_4C powders by using

https://doi.org/10.1557/jmr.2018.97 Published online by Cambridge University Press

the polymer precursor method are smaller than those synthesized by the general carbothermal reduction process. It was noted that increasing holding time resulted in producing a B_4C powder with a narrower particle size distribution (Fig. S3). This is because the number of nucleation sites increases with the well-dispersed boron and carbon sources, thus the grain growth is suppressed under low-temperature synthesis.[38] Furthermore, the particle size distribution was narrower owing to the homogeneous dispersion of nucleation sites. The mean particle size of B_4C was approximately 0.17 μm for the pyrolysis product at 600 °C for 8 h [Fig. 6(d)]. To further elucidate the particle size and structure of synthesized B_4C powders, the specific surface area, pore volume, and pore distribution of the B_4C powders were evaluated. The nitrogen adsorption–desorption isotherms indicated that all the samples showed a steep increase in isotherm at low relative pressure [Figs. S4(a), S4(c), and S4(e)], indicating the presence of micropore structures generated during the carbonization process. The presence of relative high pressures (P/P_0 = 0.45–0.97) exhibited a typical type-IV curve with a pronounced hysteresis loop and was essentially a characteristic of a mesoporous structure.[39] It was noted that the pyrolysis products of PRB after treated at 600 °C for 8 h exhibited the highest BET specific surface area (484.06 m^2/g), whereas the pore volume was 0.3699 cm^3/g. Moreover, increasing the pyrolysis temperature led to the increase in the pore diameter [Figs. S4(b), S4(d), and S4(f)]. This indicated that the produced B_4C was consisted of microporous and mesoporous structure,[40] which can also be confirmed by SEM results. As shown in Fig. 6(c), the size of the pore for the pyrolysis product was approximately 35 nm. Thus, the obtained B_4C showed great potential in the field of energy storage and catalyst carrier.[41] Further evidence for the formation of B_4C was performed by Raman spectroscopy. The narrow band appeared at 481 cm^{-1} indicated the presence of crystalline B_4C[1] (Fig. 8). The absence of two other broad bands at 1350 and 1580 cm^{-1} corresponding to the D and G (disordered and graphitic) peaks of graphite-like carbon,[42] respectively, confirmed the absence of free carbon in the B_4C powder. This was in agreement with the results found in the XRD analysis. When the holding time increased to 8 h, it is interesting to notice that the relatively higher intensity of the 806 cm^{-1} (symmetric stretching mode of boroxol rings of B_2O_3) Raman band appears in the spectra, indicating the oxidation of B_4C. Therefore, fine B_4C powder was obtained in this work from a polymeric precursor approach without a post grinding process. However, a major drawback of this method was that there still existed a little amount of residual carbon that was not removed. Rajan et al.[43] suggested that surface pretreatment during the production and processing of commercially available B_4C can easily remove many of the surface contaminants as their hydroxides. However, it was not effective in forming good coating. A potential method to remove the remaining residual carbon in the B_4C product proposed by Takano et al.[44] indicated that the free carbon can be successfully removed by applying hydrogen. Thus, potential further work of this study can be on the heat treatment of pyrolyzed samples in a hydrogen atmosphere rather than in an air atmosphere.

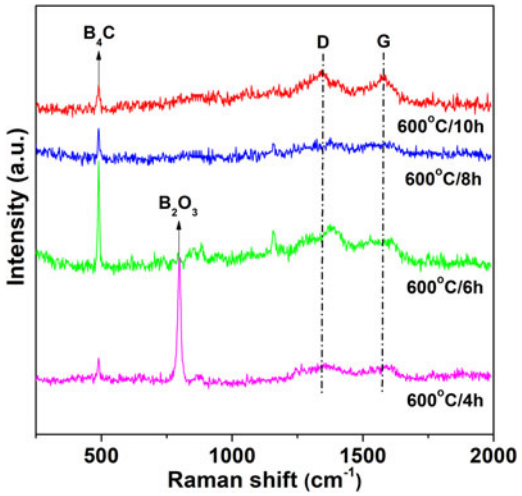


FIG. 8. Raman spectra for the pyrolysis products of PRB obtained by heat treatment at 600 °C for different durations in air after washing.

IV. CONCLUSIONS

This paper first reported the low-temperature synthesis of B_4C by using an aromatic carbon source. Compared with previous routes, the present method allows for the rapid synthesis of B_4C at a very low temperature by using low cost raw materials of resorcinol and H_3BO_3 through a simple process. By carefully analyzing the thermal pyrolysis process of PRB, the crystalline B_4C powder containing 0.82 wt% free carbon was obtained after treatment at 600 °C for 8 h. This reduction in the synthesis temperature of B_4C in this study is explained in terms of the enlarged contact surface between the B_2O_3 and carbon components. In particular, pyrolysis of the PRB precursor in air yielded C/B_2O_3 compounds with B_2O_3 particles dispersed uniformly in a carbon matrix. The morphology analysis indicated that the obtained B_4C exhibited diamond or rod-like shapes with lateral dimensions of 0.2 μm in width and 1 μm in length. Further investigation of alternative polymers can be conducted to validate the existing results before they can be considered as a possible replacement for commercially produced B_4C.

ACKNOWLEDGMENTS

This work was supported by the National Natural Science Foundation of China (Grant Nos. 51473134, 51703179, and 51273160), and Shanxi National Science Foundation (Grant No. 2017JQ5028).

https://doi.org/10.1557/jmr.2018.97 Published online by Cambridge University Press

REFERENCES

1. V. Domnich, S. Reynaud, R.A. Haber, and M. Chhowalla: Boron carbide: Structure, properties, and stability under stress. *J. Am. Ceram. Soc.* **94**, 3605 (2011).
2. I. Lopez Quintas, M. Oujja, M. Sanz, A. Benitez Cañete, R.J. Chater, M.V. Cañamares, J.F. Marco, and M. Castillejo: Micrometric rods grown by nanosecond pulsed laser deposition of boron carbide. *Appl. Surf. Sci.* **328**, 170 (2015).
3. C. Pallier, J.M. Leyssale, L.A. Truflandier, A.T. Bui, P. Weisbecker, C. Gervais, H.E. Fischer, F. Sirotti, F. Teyssandier, and G. Chollon: Structure of an amorphous boron carbide film: An experimental and computational approach. *Chem. Mater.* **25**, 2618 (2013).
4. A.K. Suri, C. Subramanian, J.K. Sonber, and T.S.R.C. Murthy: Synthesis and consolidation of boron carbide: A review. *Int. Mater. Rev.* **55**, 4 (2010).
5. A.W. Weimer, R.P. Roach, C.N. Haney, W.G. Moore, and W. Rafaniello: Rapid carbothermal reduction of boron oxide in a graphite transport reactor. *AIChE J.* **37**, 759 (1991).
6. C.H. Jung, M.J. Lee, and C.J. Kim: Preparation of carbon-free B_4C powder from B_2O_3 oxide by carbothermal reduction process. *Mater. Lett.* **58**, 609 (2004).
7. A. Jain, S. Anthonysamy, K. Ananthasivan, R. Ranganathan, V. Mittal, S.V. Narasimhan, and P.R.V. Rao: Characterization of electrodeposited elemental boron. *Mater. Char.* **59**, 890 (2008).
8. J.C. Oliveira, P. Paiva, M.N. Oliveira, and O. Conde: Laser-assisted CVD of boron carbide at atmospheric pressure. *Appl. Surf. Sci.* **138**, 159 (1999).
9. J.K. Sonber, T.S.R.C. Murthy, C. Subramanian, R.K. Fotedar, R.C. Hubli, and A.K. Suri: Synthesis, densification and characterization of boron carbide. *Bone* **46**, S64 (2013).
10. H. Zeng, Y.M. Kan, and G.J. Zhang: Synthesis of boron carbide powder from hexagonal boron nitride. *Mater. Lett.* **64**, 2000 (2010).
11. T.R. Pilladi, K. Ananthansivan, and S. Anthonysamy: Synthesis of boron carbide from boric oxide-sucrose gel precursor. *Powder Technol.* **246**, 247 (2013).
12. M. Kakiage, Y. Tominaga, I. Yanase, and H. Kobayashi: Synthesis of boron carbide powder in relation to composition and structural homogeneity of precursor using condensed boric acid-polyol product. *Powder Technol.* **221**, 257 (2012).
13. M. Kakiage, N. Tahara, I. Yanase, and H. Kobayashi: Low-temperature synthesis of boron carbide powder from condensed boric acid-glycerin product. *Mater. Lett.* **65**, 1839 (2011).
14. T.R. Pilladi, K. Ananthasivan, and S. Anthonysamy: Synthesis of nanocrystalline boron carbide from boric acid-sucrose gel precursor. *J. Mater. Sci.* **47**, 1710 (2012).
15. H. Wada, K. Kuroda, and C. Kato: Preparation of boron nitride and boron carbide by thermal treatment of boric acid-glycerin condensation product as a precursor. *J. Ceram. Assoc. Jpn.* **94**, 71 (1986).
16. A. Sinha, T. Mahata, and B.P. Sharma: Carbothermal route for preparation of boron carbide powder from boric acid-citric acid gel precursor. *J. Nucl. Mater.* **301**, 165 (2002).
17. I. Yanase, R. Ogawara, and H. Kobayashi: Synthesis of boron carbide powder from polyvinyl borate precursor. *Mater. Lett.* **63**, 91 (2009).
18. N. Tahara, M. Kakiage, I. Yanase, and H. Kobayashi: Effect of addition of tartaric acid on synthesis of boron carbide powder from condensed boric acid-glycerin product. *J. Alloys Compd.* **573**, 58 (2013).
19. M.G.L. Mirabelli, A.T. Lynch, and L.G. Sneddon: Molecular and polymeric precursors to boron-based ceramics. *Solid State Ionics* **32**, 655 (1989).
20. S. Mondal and A.K. Banthia: Low-temperature synthetic route for boron carbide. *J. Eur. Ceram. Soc.* **25**, 287 (2005).
21. G. Ferlat, A.P. Seitsonen, M. Lazzeri, and F. Mauri: Hidden polymorphs drive vitrification in B_2O_3. *Nat. Mater.* **11**, 925 (2012).
22. Y. Liu, J. Qiang, and X. Jing: Synthesis and properties of a novel hyperbranched borate. *J. Polym. Sci., Part A: Polym. Chem.* **45**, 3473 (2010).
23. S. Wang, C. Bian, B. Jia, Y. Wang, and X. Jing: Structure and thermal pyrolysis mechanism of poly(resorcinol borate) with high char yield. *Polym. Degrad. Stab.* **130**, 328 (2016).
24. S. Wang, X. Wang, B. Jia, and X. Jing: Fabrication and characterization of poly(bisphenol A borate) with high thermal stability. *Appl. Surf. Sci.* **392**, 481 (2017).
25. A. Alizadeh, E. Taheri Nassaj, and N. Ehsani: Synthesis of boron carbide powder by a carbothermic reduction method. *J. Eur. Ceram. Soc.* **24**, 3227 (2004).
26. Y. Gong, C. Fu, T. Lv, J. Chenu, Q. Zhao, and C. Li: Exploring the effect of boron and tantalum codoping on the enhanced photocatalytic activity of TiO_2. *Appl. Surf. Sci.* **351**, 746 (2015).
27. J. Wang, N. Jiang, and H. Jiang: Micro-structural evolution of phenol-formaldehyde resin modified by boron carbide at elevated temperatures. *Mater. Chem. Phys.* **120**, 187 (2010).
28. O.R. Monteiro, M.P. Delplancke Ogletree, and C.C. Klepper: Boron carbide coatings prepared by cathodic arc deposition. *J. Mater. Sci.* **38**, 3117 (2003).
29. B. Todorović-Marković, I. Draganić, D. Vasiljević-Radović, N. Romčević, M. Romčević, M. Dramićanin, and Z. Marković: Synthesis of amorphous boron carbide by single and multiple charged boron ions bombardment of fullerene thin films. *Appl. Surf. Sci.* **253**, 4029 (2007).
30. S. Wang, W. Yong, B. Cheng, Y. Zhong, and X. Jing: The thermal stability and pyrolysis mechanism of boron-containing phenolic resins: The effect of phenyl borates on the char formation. *Appl. Surf. Sci.* **331**, 519 (2015).
31. A. Kılıçarslan, F. Toptan, I. Kerti, and S. Piskin: Oxidation of boron carbide particles at low temperatures. *Mater. Lett.* **128**, 224 (2014).
32. J. Zheng, G. Shu, W. Wang, Q. Li, and W. Liu: Surface quality improvement of B_4C particles for electroless copper coating by Cu activation and oxidation roughening methods. *Appl. Surf. Sci.* **349**, 733 (2015).
33. B. Ozcelik and C. Ergun: Synthesis of boron carbide nanoparticles via spray pyrolysis. *J. Mater. Res.* **31**, 2789 (2016).
34. F.H. Gojny, M.H.G. Wichmann, U. Köpke, B. Fiedler, and K. Schulte: Carbon nanotube-reinforced epoxy-composites: Enhanced stiffness and fracture toughness at low nanotube content. *Compos. Sci. Technol.* **64**, 2363 (2004).
35. C.T. Lin, H.T. Lee, and J.K. Chen: Synthesis and characterization of molybdenum/phenolic resin composites binding with aluminum nitride particles for diamond cutters. *Appl. Surf. Sci.* **284**, 297 (2013).
36. S. Ding, S. Zheng, M. Xie, L. Peng, X. Guo, and W. Ding: One-pot synthesis of boron-doped mesoporous carbon with boric acid as a multifunction reagent. *Microporous Mesoporous Mater.* **142**, 609 (2011).
37. R. Bao and D.B. Chrisey: Short range order structure of amorphous B_4C boron carbide thin films. *J. Mater. Sci.* **46**, 3952 (2011).
38. A.W. Weimer, W.G. Moore, R.P. Roach, J.E. Hitt, R.S. Dixit, and S.E. Pratsinis: Kinetics of carbothermal reduction synthesis of boron carbide. *J. Am. Ceram. Soc.* **75**, 2509 (2010).
39. B. Krüner, P. Srimuk, S. Fleischmann, M. Zeiger, A. Schreiber, M. Aslan, A. Quade, and V. Presser: Hydrogen-treated,

https://doi.org/10.1557/jmr.2018.97 Published online by Cambridge University Press

sub-micrometer carbon beads for fast capacitive deionization with high performance stability. *Carbon* **117**, 46 (2017).
40. C. Nita, M. Bensafia, C. Vaulot, L. Delmotte, and C.M. Ghimbeu: Insights on the synthesis mechanism of green phenolic resin derived porous carbons via a salt-soft templating approach. *Carbon* **109**, 227 (2016).
41. T.Y. Ma, L. Liu, and Z.Y. Yuan: Direct synthesis of ordered mesoporous carbons. *Chem. Soc. Rev.* **42**, 3977 (2013).
42. F. Tuinstra and J.L. Koenig: Raman spectrum of graphite. *J. Chem. Phys.* **53**, 1126 (1970).
43. J.P. Deepa, V.G. Resmi, T.P.D. Rajan, C. Pavithran, and B.C. Pai: Studies on the influence of surface pre-treatments on electroless copper coating of boron carbide particles. *Appl. Surf. Sci.* **257**, 7466 (2011).
44. M. Takano, A. Itoh, M. Akabori, and T. Ogawa: Oxygen solubility in dysprosium mononitride prepared by carbothermic synthesis. *J. Alloys Compd.* **327**, 235 (2001).

Supplementary Material

To view supplementary material for this article, please visit https://doi.org/10.1557/jmr.2018.97.

https://doi.org/10.1557/jmr.2018.97 Published online by Cambridge University Press